Earthq Eng & Eng Vib (2021) 20: 127-139 **DOI**: https://doi.org/10.1007/s11803-021-2010-2

Seismic collapse simulation of existing masonry buildings with different retrofitting techniques

Ge Dongdong[1†], Du Chunbo[2‡], Miao Qisong[3§] and Chen Xi[3§]

1. *College of Architecture and Civil Engineering, Beijing University of Technology, Beijing 100124, China*
2. *Key Laboratory of Earthquake Engineering and Engineering Vibration, Institute of Engineering Mechanics, China Earthquake Administration, Sanhe 065201, China*
3. *Beijing Institute of Architectural Design, Beijing 100045, China*

Abstract: Masonry buildings are primarily constructed out of bricks and mortar which become discrete pieces and cannot sustain horizontal forces created by a strong earthquake. The collapse of masonry walls may cause significant human casualties and economic losses. To maintain their integrity, several methods have been developed to retrofit existing masonry buildings, such as the constructional RC frame which has been extensively used in China. In this study, a new method using precast steel reinforced concrete (PSRC) panels is developed. To demonstrate its effectiveness, numerical studies are conducted to investigate and compare the collapse behavior of a structure without retrofitting, retrofitted with a constructional RC frame, and retrofitted with external PSRC walls (PSRCW). Sophisticated finite element models (FEM) were developed and nonlinear time history analyses were carried out. The results show that the existing masonry building is severely damaged under occasional earthquakes, and totally collapsed under rare earthquakes. Both retrofitting techniques improve the seismic performance of existing masonry buildings. However, it is found that several occasional earthquakes caused collapse or partial collapse of the building retrofitted with the constructional RC frame, while the one retrofitted by the proposed PSRC wall system survives even under rare earthquakes. The effectiveness of the proposed retrofitting method on existing masonry buildings is thus fully demonstrated.

Keywords: existing masonry structure; seismic retrofit; collapse simulation; PSRCW; nonlinear time history analysis

1 Introduction

A large number of masonry buildings collapsed during the 2008 Wenchuan earthquake and 2009 Yushu earthquake, which caused many casualties and property losses. It was found that the material mechanical properties of these buildings were significantly degraded due to the effects of aging. More importantly, seismic strengthening measures were lacking. Masonry buildings are primarily constructed by bricks and mortar. As the major aseismic member, the masonry wall works monolithically to resist small to medium earthquakes. However, the masonry wall becomes discrete pieces once cracks develop when subjected to a rare earthquake (Sun and Yan, 2015). Although the friction along the cracks dissipates the seismic energy during in-plane deformation, collapse can easily occur when out of the plane.

To maintain integrity, several methods have been developed to retrofit existing masonry buildings (Taghdi *et al*., 2000; ElGawady *et al*., 2004; Moon *et al*., 2007; Gu *et al*., 2012; Charleson and Blondet, 2012). The constructional RC frame is one effective method that was developed forty years ago and has been extensively used in China, particularly after the Tangshan earthquake (Cai, 1984) and Wenchuan earthquake (Chen, 2009). The constructional RC frame is configured with constructional columns and ring beams. The constructional RC columns are commonly constructed at the joints of lateral and longitudinal walls, while the ring beams are often built along the edges of the story floors. The constructional columns and the ring beams form the RC frame attached externally to the existing masonry building. The confinement effect improves the integrity of the existing masonry building. However, the stiffness of the RC frame does not ensure the safety of all masonry walls. Partial collapses have been observed during the 2013 Lushan earthquake (Dai

Correspondence to: Du Chunbo, Key Laboratory of Earthquake Engineering and Engineering Vibration, Institute of Engineering Mechanics, CEA, Yanjiao, Sanhe 065201, China
Tel: +86-316-3395222
E-mail: duchunbo_iem@163.com
†Post-doctor; ‡Master Candidate; §Senior Engineer

Supported by: Scientific Research Fund of Institute of Engineering Mechanics, CEA under Grant No. 2016A06, National Key R&D Program of China under Grant Nos. 2016YFC0701101 and 2017YFC1500701, and National Natural Science Foundation of China under Grant No. 51678538
Received January 6, 2019; **Accepted** June 6, 2019

et al., 2013). In this study, a new method using precast steel reinforced concrete (PSRC) panels is developed. The PSRC panels are built up as an external PSRC wall (PSRCW) system surrounding and well connected to the existing masonry building, which provide enough confinement to effectively improve the ductility, strength, and stiffness of old masonry structures. A full-scale five-story retrofitted building has been demonstrated effective by use of online hybrid tests (Wang *et al*., 2012, 2013). As shown in Fig. 1, it is a two-bay by two-span, five-story full-scale building with a width of 6.2 m, length of 9.5 m, and height of 14.2 m. The height of the first story is 3.0 m, while the rest of the stories have a height of 2.8 m. It was retrofitted by the PSRCW method. The test was stopped before the structure collapsed due to the capacity limitation of the loading facilities, and it was also deemed very dangerous in the lab environment. The structural collapse resistance under more ground motions with larger PGA can be analyzed by numerical simulation and the collapse behavior of the retrofitted structure can be evaluated in terms of fragility. In addition to constructional RC frame and PSRCW, there are several other strengthening methods such as coating cement mortar with steel meshes, coating polymer mortar with steel strand meshes and concrete splints and so on. However, most of these methods are based on on-site pouring or shotcrete construction which creates a long period for construction and residents must move elsewhere. In addition, the usable area is reduced after wall thickening, which makes the usable space much smaller.

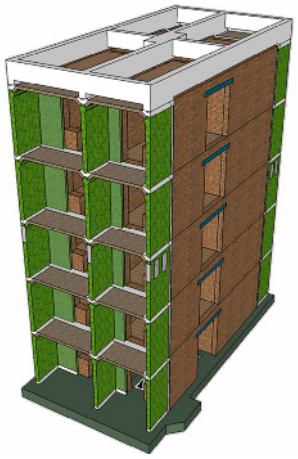

Fig. 1 Full-scale five-floor retrofitted masonry building

This study continues to examine the collapse behavior of the retrofitted building in terms of fragility. A comparative numerical study is conducted to compare the collapse behavior of three structures, i.e., the structure without retrofitting, the structure retrofitted by the constructional RC frame, and retrofitted by the external PSRC walls (PSRCW), simply called a unreinforced masonry (URM), constructional RC frame, and PSRCW, respectively. The FEM model is constructed by ABAQUS, where a user-developed element removal technique is incorporated. The collapse behavior of the three structures is examined by incremental dynamic analysis (IDA). The damage and collapse modes are identified, and the influence on the ductility is discussed.

2 Prototype and retrofitting technologies

2.1 Prototype

The prototype building was built forty years ago. It has five stories, and the total height is 15.0 m. Dimensions are shown in Fig. 2. The external masonry walls are typically 370 mm thick to provide warmth during the winter, while the interior walls have a thickness of 240 mm. On the top of the windows or doors, there are RC concrete lintels to sustain the overhead walls. Precast hollow slabs were used to construct the floor system. The thickness is 130 mm for the floor, and 180 mm for the roof. All precast hollow slabs were supported on two transversal walls at both ends. The support length is approximately 50 mm. Once all the precast hollow slabs were positioned, a layer of plain concrete with the thickness of 50 mm was poured on top to integrate all separated precast hollow slabs.

Only transverse walls bear the weight. However, there are no seismic specifications for this masonry building. The construction material of masonry walls has been aging for a long time, and the mechanical properties had significantly degraded. According to the on-site sampling and measurement, the strength of the

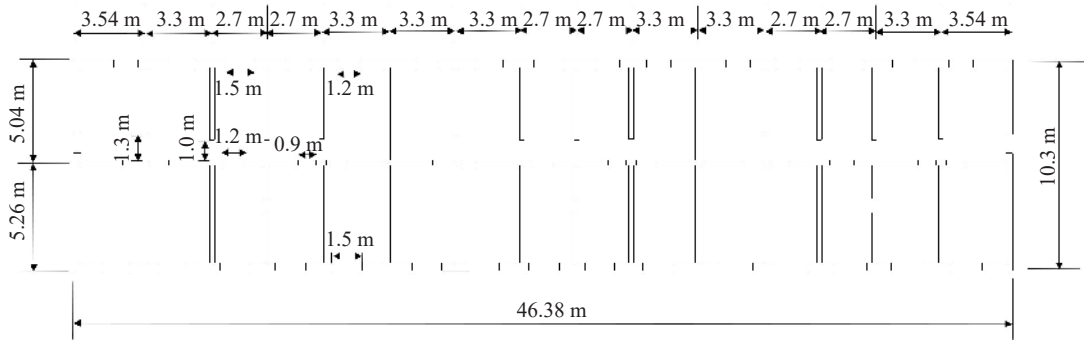

Fig. 2 Floor plan of prototype building

bricks is only about 7.5 MPa, and the strength of the mortar is approximately 2.5 MPa in the bottom three stories and 1.0 MPa in the rest of the stories. These values were adopted in numerical modeling. All the materials are classified according to the Chinese "Code for design of masonry structures" (GB 50003-2011, 2011). Refer to Table 1 in Chapter 3.1 for their nominal mechanical properties. The seismic assessment results show that this building is not strong enough to resist potential earthquakes in the residual life periods of 30 years.

2.2 Retrofitted structure by constructional RC frame

Once the pure masonry structure is confined by existing methods, such as an externally attached RC frame, its ductility is significantly improved. The attached RC frame features a lower rebar ratio and smaller cross-section than in a traditional RC frame. Therefore, it is commonly called a constructional RC frame, consisting of constructional columns and ring beams. The constructional column is often set at the joint connecting the transversal and longitudinal walls. A well-connected constructional column helps to improve the integrity of the masonry structure system. The ring beam is set around the building at each floor level, which is supposed to enhance the connection between the masonry walls and the precast hollow slabs. When used as the retrofitting technique, the constructional RC frame is externally attached to the masonry building. Some steel tie rods are often employed to connect the frame on the opposite sides of the building. They are deployed along the internal transversal walls and function as the internal ring beam. With this confinement, the ductility of the overall building is improved.

In this specific application, one constructional column is set at each connection of the external longitudinal walls and transversal walls, as shown in Fig. 3. The ring beam is constructed at the floor level, and is also connected externally to the external surface of the building. In this study, the cross-sections of the constructional columns and beams are all 240 mm × 240 mm, with a longitudinal rebar ratio of 1.0%. The concrete is C30 with the nominal mechanical properties listed in Table 1. A pair of Q235 steel tie rods with the diameter of 16 mm are used to connect the constructional RC frames on both sides of the transverse walls. Due to the inconvenient indoor construction of the ring girder, the Q235 tie rods serve the role of a ring beam, which can be used to tie masonry cross walls together to enhance the integrity of the structure. They are located along each internal transversal wall. The ring beams and steel tie rods are set for all stories, as shown in Fig. 2.

2.3 Retrofitted structure by PSRCW

The retrofitting method using the constructional RC frame demands a lot of in-situ work. To reduce the adverse effect on living environment, a new method using PSRC panels was developed (Li *et al.*, 2017). The PSRC panels are securely attached to the external surface in the longitudinal direction, while in the transversal direction, the PSRCW are assembled together with the prefabricated slabs to form an external balcony at each side of the building. The embedded steel members in the wall panels serve as boundary members to prevent premature failure at the wall feet, and provide

Table 1 Parameters to define backbone curve of employed materials

Material	Elastic modulus	Compressive yield strength	Compressive ultimate strength	Tensile yield strength	Tensile ultimate strength
MU7.5, M2.5	1.93×10^3	2.09	0.02	0.13	0.01
MU7.5, M1.0	1.09×10^3	1.10	0.01	0.12	0.01
C30	3.0×10^4	20.1	4.0	2.01	0.2
Q235	2.0×10^5	235	350	235	350
HRB400	2.0×10^5	400	550	400	550

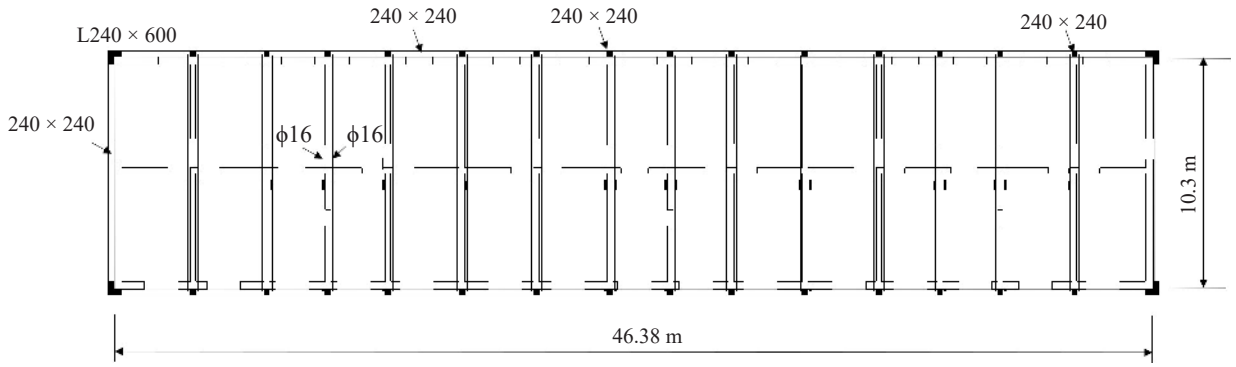

Fig. 3 Floor plan of the constructional RC frame

a connection between the walls in adjacent stories. The steel members are responsible for transferring the bending and shear force. In this way, two external shear wall structures are constructed around the existing masonry building, which are further connected by RC girders above the roof. Therefore, the RC part forms a huge frame enwrapping the masonry frame. With the confinement effect from the external RC balcony, it is expected that the failure mode of the entire building would change from direct shear failure to the more ductile bending-shear mixed failure mode. The key to the proposed retrofitting technology is to ensure the connection and collaboration between the panels and the existing masonry building. Three techniques are developed to connect the RC balcony tightly with the existing masonry walls, namely "reinforced concrete (RC) keys", "implanted reinforcement" and "CSV cement", as shown in Fig. 4. The RC keys and implanted reinforcement are implemented first, followed by grouting materials. The performance of these three techniques have been verified in the connection between the panels and the existing masonry building (Li *et al.*, 2017).

In this study, the retrofitting design using PSRCW is shown in Fig. 5. The PSRCW with the thickness of 130 mm are pasted along the two external longitudinal walls by the three connection techniques mentioned above. Previous experiments demonstrated that the connection was very tight and little damage was observed after very-rare earthquake excitation (Li *et al.*, 2017). In the transversal direction, the PSRCW with a thickness of 200 mm are employed. They are 1.35 m long on one side and 1.5 m on the other. The reinforcement ratio of the PSRCWs is 0.3%. Shaped steels are set at both sides of the transverse wall as the structural boundary members. The thickness of the balcony RC slabs is 120 mm. The girder above the roof has a cross-section of 240 mm × 240 mm with six 16 mm steel rebars in diameter. There is one girder above each piece of transversal masonry wall. The head walls at both ends of the building are all enhanced with a 40 mm thick steel mesh mortar. The concrete in the wall and slab panels are all C30, the shaped steels are Q235, and the reinforcement rebars are all HRB400. Detailed information about the cross-sections can be found in the previous study (Li *et al.*, 2017).

3 Finite element models

The discrete element method (DEM) and finite element method (FEM) are two commonly used

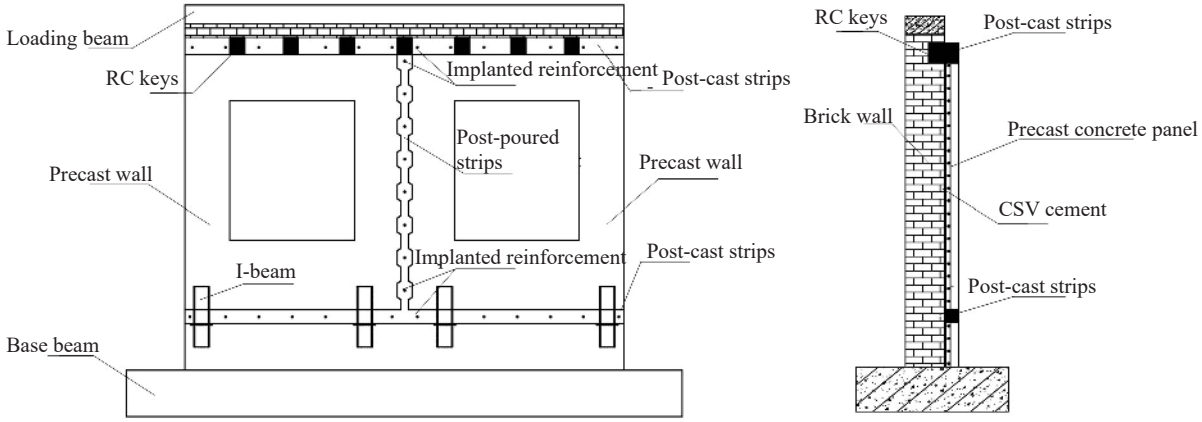

Fig. 4 Main techniques in construction of PSRCW

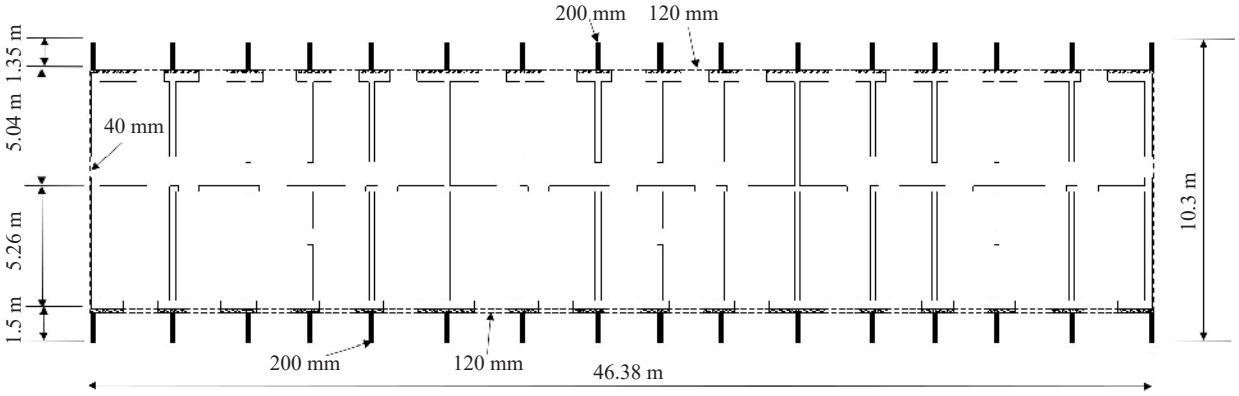

Fig. 5 Floor plan of PSRCW

methods in simulating the collapse behavior of masonry buildings. Several studies (Hakuno and Meguro, 1993; Lemos, 2007; Caliò *et al*., 2012) adopted DEM. The definition of spring elements between rigid blocks is the key to accurately reproduce the initiation of damage through collapse of a masonry structure. However, it is difficult to reasonably provide the mechanical properties of these springs. Therefore, the accuracy of DEM is often limited. FEM, once combined with the element removal technique, is able to simulate the collapse behavior of structures (Xu, 2008). Zheng (2012) employed the commercial software LS-DYNA to study the bearing force and the collapse pattern with respect to the design parameters by use of the incremental dynamic analyses. In LS-DYNA, the first-order elements are mostly applied to accelerate the computation speed, while the accuracy is often low because the number of sectional integration points is insufficient. Moreover, the plasticity is not adequately considered by LS-DYNA. Most previous studies (Li, 2013) often chose solid elements to model the beam and column components in masonry buildings, which are either inaccurate to reproduce the sectional behavior or inefficient because of the large number elements. Meanwhile, solid elements are not suitable to simulate the wall-type components either because more solid elements need to be divided in the cross-section direction. It is more feasible to establish a refined 3D FEM model by fiber-based beam elements to simulate the RC beam and column components and the composite layered shell elements for masonry walls.

3.1 Finite element modeling

To efficiently simulate the collapse behavior of a masonry building, the continuum finite element model is developed by using commercial software called ABAQUS. In this model, the masonry wall is treated as an isotropic and homogeneous continuum member in which the interaction between the blocks and mortar is neglected. However, the failure mechanisms of the mortar joint failure, block fracture, block slippage, and so on, cannot be distinguished. Instead, it relies upon a suitable material model with specific constitutive relations and the failure criterion to reproduce the global behavior of masonry walls. Therefore, it is more suitable to model the overall masonry structure.

ABAQUS is equipped with a shell element with a composite layered section, where concrete, rebar layers, and masonry can be incorporated into a single section with multiple layers along the thickness, as shown in Fig. 6. Different material models are assigned to the specific layer in various directions so that the plate-type structural member with distinct characteristics in both in-plane directions can be simulated. Along the thickness, the plane-keep-plane assumption is adopted, and the sectional forces are integrated linearly according to the response of each layer. In the plane directions, linear interpolation functions are used in both directions, and the reduced integration technique is employed to reduce the computational effort. To maintain the accuracy, a wall member is meshed at least four elements in one direction. In this study, both the masonry wall and retrofitted masonry wall either by steel reinforced concrete (SRC) panels or by steel mesh mortars, and the RC slabs are simulated by the composite shell element.

Line-type members, such as constructional columns, ring beams and shaped steels in the SRC panels, are represented by beam elements based on the Timoshenko theory considering the associated shear behavior. Each constructional RC column or ring beam is simulated by two Timoshenko beam elements, one representing the concrete material and the other for the steel rebars. Two beam elements share nodes and have the same shape function. The deformation of different material fibers at the same position of the cross section is consistent with each other, as shown in Fig. 7. The steel tie rods are represented by truss elements. When constructing the model, each beam or column member will be meshed in the same way as the wall member along the axial direction of the beam element.

Both concrete and mortar are represented by the

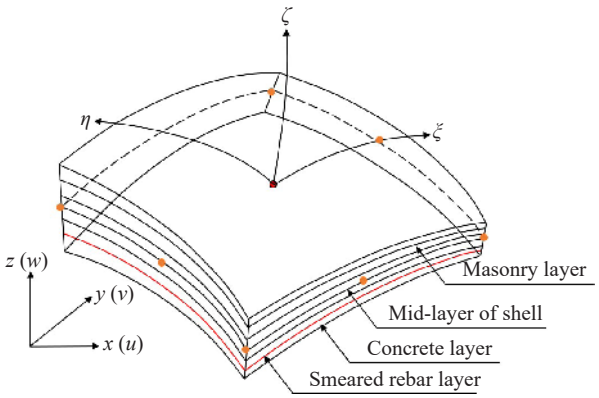

Fig. 6 Finite elements to represent members with composite sections

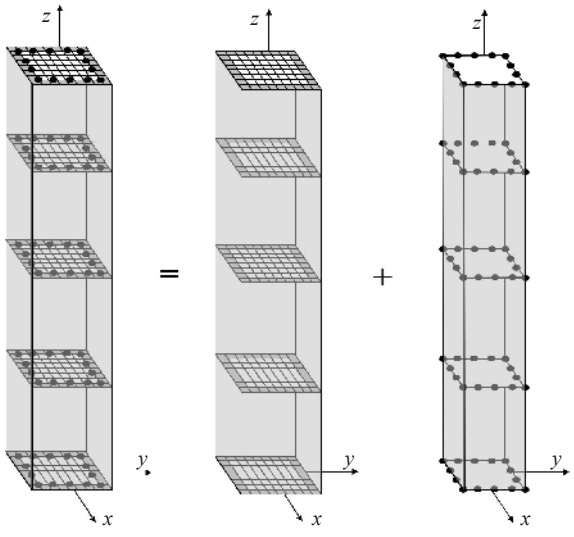

Fig. 7 Finite elements to represent RC beam element with two beam elements shear nodes

Concrete Damaged Plasticity (CDP) constitutive model provided by ABAQUS, which is able to consider the difference between the tension and compression strength, and the degradation of stiffness and strength under the cyclic loading. Both compression and tension would result in damage to the concrete. Once the concrete is damaged, the stiffness cannot recover. This mechanism is simulated by the tensile damage factor d_t and compressive damage factor d_c for the tension and compression, respectively, which are defined as a function of the plastic strain. The compressive damage factor d_c is zero at the elastic stage, while increases quickly once it enters the plastic stage. When reaching the peak compressive strength, the compressive damage factor is empirically selected from 0.2 to 0.3. The damage plasticity model provided by ABAQUS is particularly suitable for 2D or 3D elements, but not for the 1D line-type elements. To this end, a uniaxial material for concrete is developed and incorporated into ABAQUS by the VUMAT subroutine. The backbone curves of the CDP models for the concrete and mortar are given in Fig. 8 where standard strength values are employed as discussed in Appendix C in the "Code for design of concrete structures" (GB 50010-2010, 2010). The damage factors are also plotted in Fig. 9, which are determined empirically. All steel members, including shaped steels, rods, and rebars, are all simulated by a uniaxial bilinear model with kinematic hardening rule without any degradation, so that the rebar slippage inside the concrete cannot be modeled.

3.2 Collapse simulation by element deactivation and contact definition

During the earthquake, the masonry often suffers local failure first, which continuously results in damage of the adjacent components and finally the complete failure of the structure; meanwhile, the overall continuous structure changes into discrete parts (Lu *et al.*, 2013). To simulate this situation, both fiber beam elements and composite layered elements are used in this study with

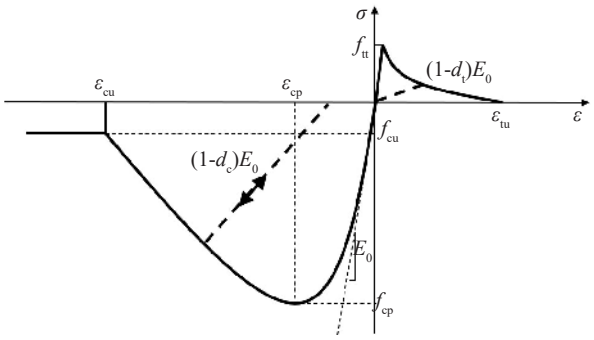

Fig. 8 Backbone curve of concrete and masonry materials

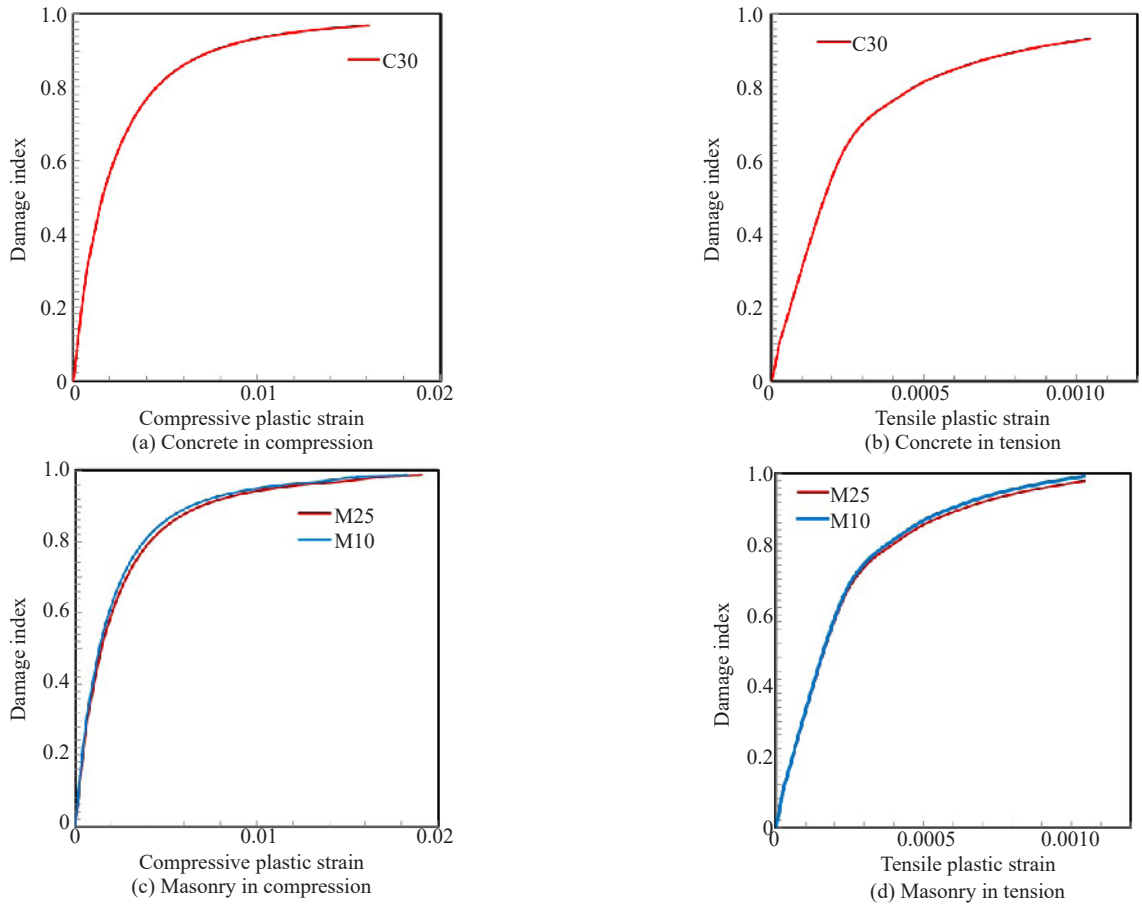

Fig. 9 Damage factors for concrete and mortar

sophisticated stress-strain constitutive laws. The failure of the element is realized through checking the strain of each Gauss integration point in one element. If the strain exceeds the critical value, this integration point is deactivated. Once all integration points in one element stop from the analysis, this element is actually removed.

RC columns and beams are modeled by fiber beam elements, in which there is one integration point in the longitudinal direction and multiple integration points to describe the shape of the cross sections. The failure criterion for rebar is that the compressive strain of the integration point exceeds 0.01 or the tensile strain exceeds 0.1, corresponding to rebar compressive buckling and tensile rupture, as given in Table 2. A very low tensile strength is assigned to the concrete material and most tensile stress is sustained by rebars. The concrete sustains mainly compression and fails at the critical compressive strain of 0.0033 (GB 50010-2010, 2010).

Masonry walls, concrete walls and composite walls are all modeled by composite layered shell elements which have 21 integration points (42 integration points in composite walls) in the thickness direction and four integration points in the plane direction. In this study, the masonry and concrete materials are both simulated by the damaged plasticity model. The associated stiffness and strength degradation approximately simulate the diminishing of the element, while the residual shear strength affects the simulation results of collapse. Therefore, a more rational method of element deactivation should be developed and the strain-based deactivation method has been developed. The strain thresholds for masonry walls under compression, tension and shear failure are 0.01, 0.01 and 0.003, respectively. The compressive strain threshold value of concrete in the composite layered shell element is 0.01 considering the definition of the damaged plasticity model.

If all integration points in a composite layered shell element are deactivated, this element is actually removed from the model. In this case, the mass associated with this element also disappears which would result in a distortion of the actual situation because most of the mass is distributed on the walls and slabs. Meanwhile, the complete removal of one element changes the stress field of adjacent elements suddenly. The stable time increment will be decreased sharply, causing low calculation efficiency and even the failure to analysis because of the damaged plasticity model. To solve this problem, this study proposed a pseudo rebar layer method, as shown in Fig. 8. The pseudo rebar layer with limited elastic modulus of 2.0 MPa and 10 mm diameter is placed parallel to the masonry layered shell element, and the integration points of the pseudo rebar layer are not removed. Therefore, after all the integration points of concrete and masonry layers are deactivated, the pseudo rebar layer can still provide additional integration points to avoid the entire element removal while its effect on the structural behavior is limited.

During the collapse simulation, the component debris has a significant impact on the substructural damage. It

Table 2 Critical strain for checking integration point failure

Element type	Material	Critical compressive strain	Critical tensile strain	Critical shear strain
Fiber beam element	Concrete	0.0033	/	/
	Rebar	0.01	0.10	/
Composite layered shell element	Masonry	0.01	0.01	0.003
	Concrete	0.01	/	0.003
	Rebar	0.01	0.10	/

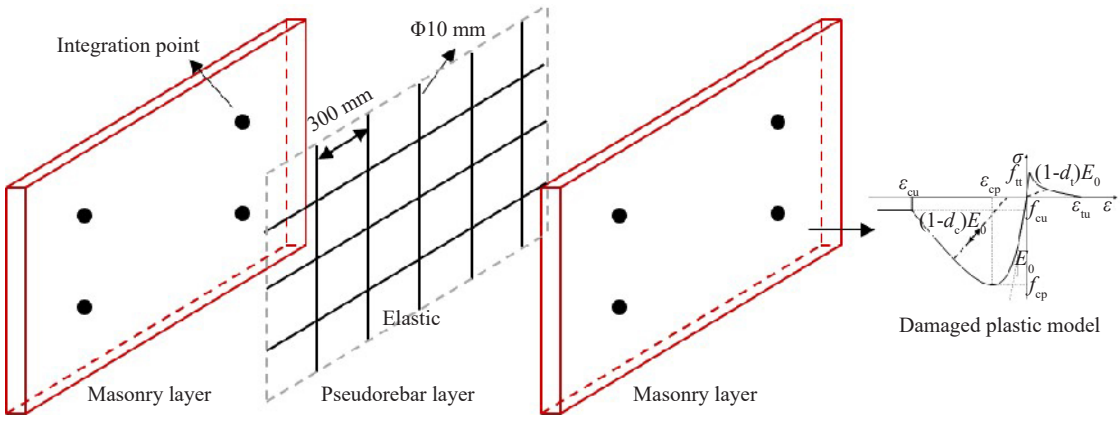

Fig. 10 Masonry layer shell element with inner pseudo rebar layer

is thus necessary to define the contact relationship in the model. The collision among the elements during the collapse process is often simulated through the self-collision in ABAQUS. The explicit finite element method can be used to search the element contact efficiently, and the contact force can be calculated by the penalty function or Lagrange multiplier method. To ensure the validity and correctness of the contact, all boundary meshes must be coordinated.

3.3 Collapse margin analysis using IDA

Structural collapse is a very complicated nonlinear process. In this study, the criterion for collapse is when the local or global vertical bearing capacity is lost. To find the adequate collapse margin of a structure, the incremental dynamic analysis (IDA) is often employed according to FEMA P695, allowing the structure to gradually develop plasticity so that different collapse modes under a variety of earthquake input motions can be comprehensively examined (Vamvatsikos and Cornell, 2002). FEMA P695 (2009) defines the Collapse Margin Ratio (CMR) as the value of the actual seismic collapse resistance of structures over the demand. Considering the difference between ground motions, IDA analysis of structures should be based on a large number of ground motions (the total number of ground motions counted as N_{total}). By gradually increasing the intensity of ground motions, and recording the number of collapse N_{collapse} under a certain intensity of the earthquake, $N_{\text{collapse}}/N_{\text{total}}$ can be obtained as the collapse probability of the structure under a given intensity of ground motion (Collapse Possibility). With the increase of earthquake intensity, the probability of collapse will also increase. Thus, the relationship curve between earthquake intensity and the probability of collapse can be obtained. This curve is called the Collapse Fragility Curve of structures, which provides a more scientific method for evaluating the collapse resistance of structures.

Taking the acceleration spectrum value $S_a(T_1)$ as an index of ground motion intensity, the intensity, at which the structure collapses in 50% probability of all the working conditions, is denoted as the averaged collapse resistance of the structure. CMR is the ratio between the averaged collapse resistance over the intensity of the maximum credible earthquake (MCE), as given in Eq. (1) where T_1 is the fundamental period of the structure.

$$\text{CMR}=\frac{S_a(T_1)_{50\%\text{collapse}}}{S_a(T_1)_{\text{MCE}}} \tag{1}$$

Note that different intensities of ground motion can also be used. In order to compare the collapse resistance of different structures, i.e., unreinforced masonry, constructional RC frame, and PSRCW, the peak ground acceleration (PGA) is used in this study instead, which is also adapted to Chinese seismic code.

3.4 Selection of ground motions

The target structure was constructed on a site with the soil type II, and the seismic fortification intensity of 0.2 g in PGA (GB 50011-2010, 2016). The residual life of the building is 30 years, shorter than that of a new construction building, which is 50 years. Therefore, the intensities used for the time history analyses shall be updated as 0.15 g according to the "Seismic ground motion parameters zonation map of China (GB 18306-2015, 2015)". The selection of ground motion is very important for collapse margin analysis. The FEMA P695 report recommends no less than 20 seismic records for analysis to cover different characteristics of earthquakes. Considering that the location of the studied building is close to the epicenters from previous earthquakes, 21 representative near-field ground motions were selected for the IDA analysis, which are recommended by FEMA P695 and collected from the PEER NGA database, as listed in Table 3. The first eleven motions feature pulse-like components, while the rest do not. Their acceleration response spectra are shown in Fig. 11 and compared with the Chinese design spectra.

4 Simulation results and discussion

The components of seismic waves are input in three directions with the PGA ratio of 1.00:0.85:0.65 for the two horizontal directions and the vertical direction. Two cases are considered, where the principal component of one set of ground motions is assigned to the x and y directions of the building, respectively. In IDA analysis, the PGA in the principal direction starts from 0.125 g, increasing by 0.025 g until 0.55 g. The gravity is imposed before the time history analysis and the gravity acceleration was held for 6 s to damp out the free vibration. The Rayleigh damping is adopted and damping ratios of 0.05 are assigned to the first two vibration modes.

4.1 Natural periods

The periods of the first six vibration modes of the three structures are listed in Table 4. The first three

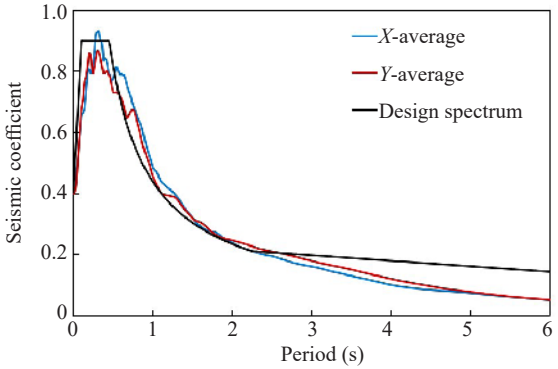

Fig. 11 Response spectra of 21 motions

modes are primarily in the *X*-, *Y*-directions and torsion about the *Z*-axis, respectively. The retrofitting technique using constructional RC frame slightly improves the overall stiffness, while the method using PSRCW significantly increases the overall stiffness by 230% in the *Y*-direction, 170% in the *X*-direction, and 190% in the torsional direction about the *Z*-axis.

4.2 Structural damage patterns

The No. 20 ground motion has concentrated energy in high frequencies close to the masonry structure. Figure 12 shows a typical collapse mode of the unreinforced masonry under this motion with the PGA of 0.175 g, where the blue element represents the wall with removal of integral points, while the red one shows the integral points that survived. At 10.95 s, part of the lintels of the longitudinal wall were damaged, and the middle transversal wall at the bottom was destroyed, which is consistent with the shear failure observed in recent earthquake disasters. At 11.95 s, the bottom walls on the left side of the structure were further aggravated, and at 12.25 s, several bays were seriously damaged, implying partial collapse. From 12.25 s to 13.20 s, the collapse region extended the two head walls. At 13.50 s, the overall structure completely collapsed, and the maximum vertical displacement on the left side of structure reached 6 m.

Under the same ground motion and intensity, the collapse of the constructional RC frame was also

Table 3 Summary of PEER NGA database information and parameters of recorded ground motions for the near-field record set

ID No.	Record No.	Earthquake magnitude	Year	Earthquake name	PGA_{max} (g)	PGV_{max} (cm/s)
1	181	6.5	1979	Imperial Valley-06	0.44	111.9
2	182	6.5	1979	Imperial Valley-06	0.46	108.9
3	292	6.9	1980	Irpinia, Italy-01	0.31	45.5
4	723	6.5	1987	Superstition Hills-02	0.42	106.8
5	802	6.9	1989	Loma Prieta	0.38	55.6
6	821	6.7	1992	Erzican, Turkey	0.49	95.5
7	828	7.0	1992	Cape Mendocino	0.63	82.1
8	1063	6.7	1994	Northridge-01	0.87	167.3
9	1086	6.7	1994	Northridge-01	0.73	122.8
10	1165	7.5	1999	Kocaeli, Turkey	0.22	29.8
11	1605	7.1	1999	Duzce, Turkey	0.52	79.3
12	126	6.8	1976	Gazli, USSR	0.71	71.2
13	160	6.5	1979	Imperial Valley-06	0.76	44.3
14	495	6.8	1985	Nahanni, Canada	1.18	43.9
15	496	6.8	1985	Nahanni, Canada	0.45	34.7
16	741	6.9	1989	Loma Prieta	0.64	55.9
17	753	6.9	1989	Loma Prieta	0.51	45.5
18	825	7.0	1992	Cape Mendocino	1.43	119.5
19	1004	6.7	1994	Northridge-01	0.73	70.1
20	1048	6.7	1994	Northridge-01	0.42	53.2
21	1176	7.5	1999	Kocaeli, Turkey	0.31	73

Table 4 First six natural periods (units: s)

Mode order	Unreinforced masonry	Constructional RC frame	PSRCW	Mode description
1	0.41	0.39	0.25	1st *X*
2	0.31	0.27	0.17	1st *Y*
3	0.29	0.26	0.17	1st *Z* torsion
4	0.17	0.15	0.12	2nd *Z* torsion
5	0.14	0.14	0.08	2nd *X*
6	0.11	0.09	0.08	2nd *Y*

observed in Fig. 13. The damage also initiated from the lintel over the window in the longitudinal walls. But more damage was concentrated in the transversal wall thereafter. At 14.50 s, most elements in the transversal walls were stopped in the model. The structure collapsed at 15.23 s when the maximum vertical displacement reached 0.50 m. Compared with the unreinforced masonry, the retrofitting delayed the collapse for about 1.5 s.

The collapse resistance of the PSRCW has been significantly improved. As shown in Fig. 14, the structure did not collapse until the intensity reached 0.45 g. Although most masonry elements were removed, the PSRCW remained. Since the transversal walls sustained the most gravity, they suffered more damage than the longitudinal walls.

4.3 Displacement responses and base shear forces

The displacement responses to the No. 13 ground motion are compared for the three structures at a PGA of 0.175 g, as shown in Figs. 15 and 16 for the X and Y directions, respectively. It can be seen that the displacement response of the PSRCW reinforced structure is minimum, meaning that the reinforcement effect is very efficient. The displacement response at

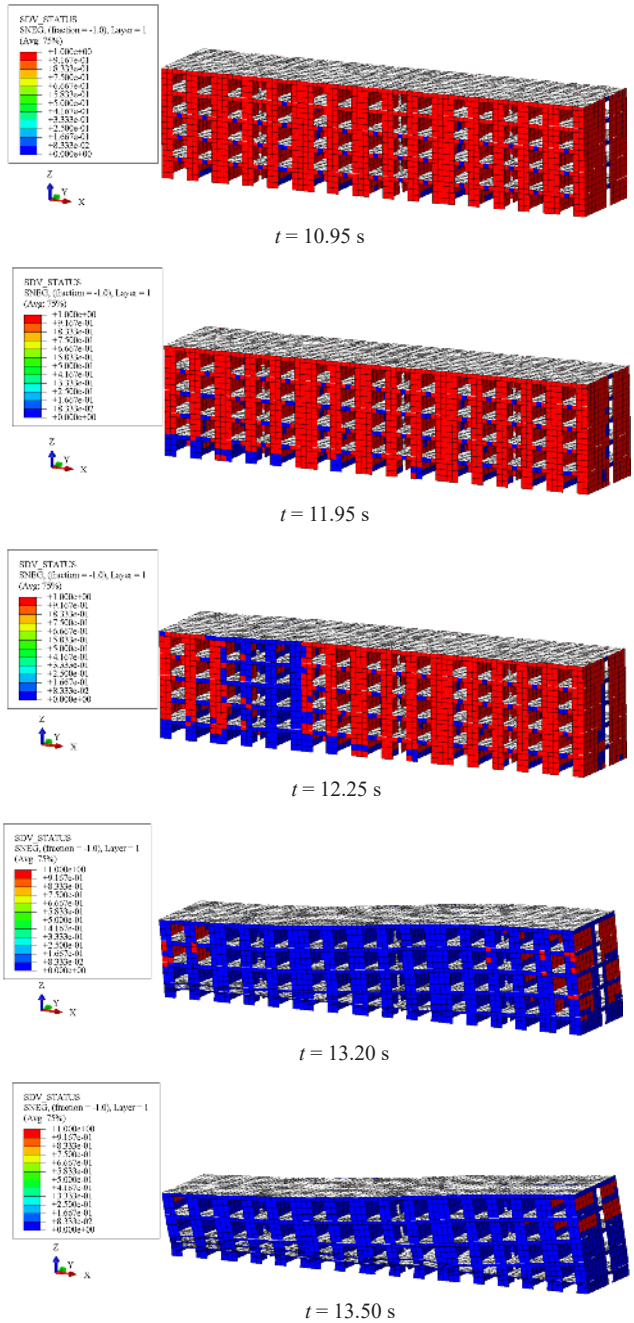

Fig. 12 Damage and collapse of unreinforced masonry for different duration of the earthquake at 0.175 g

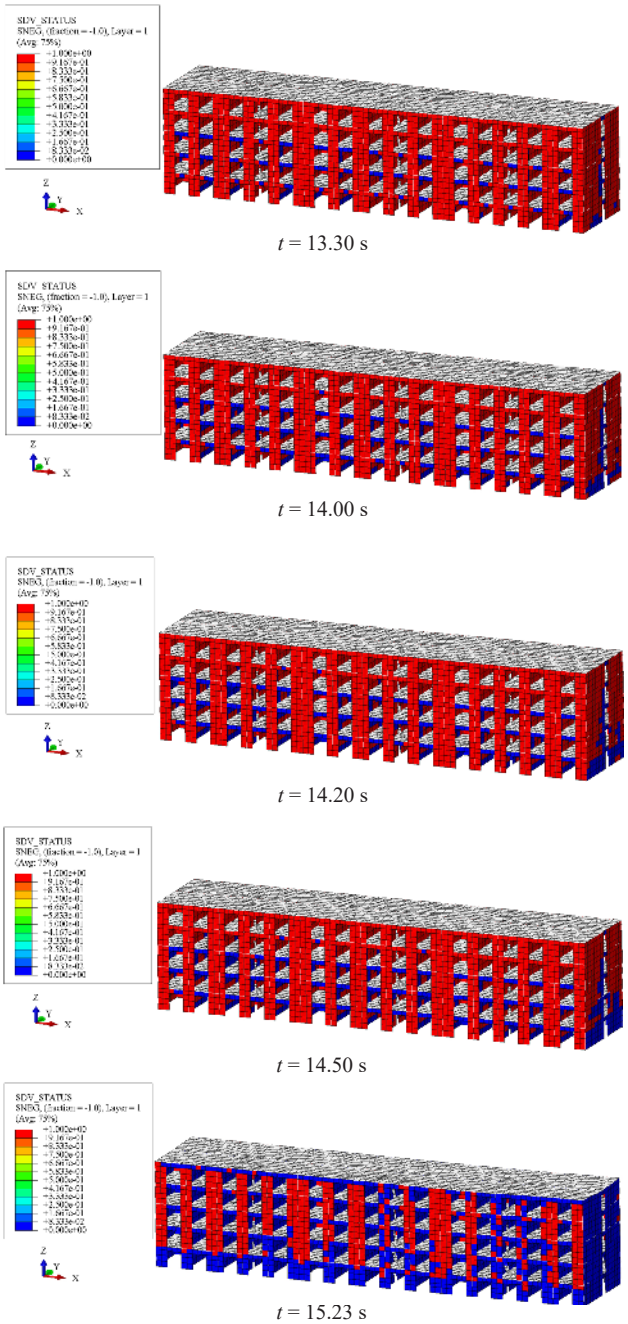

Fig. 13 Damage and collapse of constructional RC frame for different duration of the earthquake at 0.175 g

the first floor of the constructional RC frame reinforced structure is larger than that of unreinforced masonry. However, the top floor displacement response is smaller. Generally, the retrofitting effect is not as pronounced. Similar phenomenon can also be observed in the *Y*-direction.

The inter-story drift ratios in the *X*-direction are listed in Table 5. The maximum inter-story drift ratio of unreinforced masonry is 1/270 in the third story. For the constructional RC frame, the maximum value is 1/254 in the first story. Similar drift demands in these two structures again implies the limited effect of retrofitting. Based on a large number of experimental results collected by Su *et al.*, the inter-story drift ratio of 1/150 was assigned as the limit of "collapse failure" for masonry structure with ring beams and constructional columns, while for the unreinforced masonry structures, when the inter-story drift ratio reaches 1/200–1/300, the structure is on the verge of collapse. Therefore, the unreinforced masonry suffered collapse, while the constructional RC frame has a margin to collapse, although very limited. For the PSRCW, the maximum value is 1/1547 in the second story, much smaller than the previous two cases. Therefore, the masonry structure would be well protected.

The retrofitted structure first collapsed in the *Y*

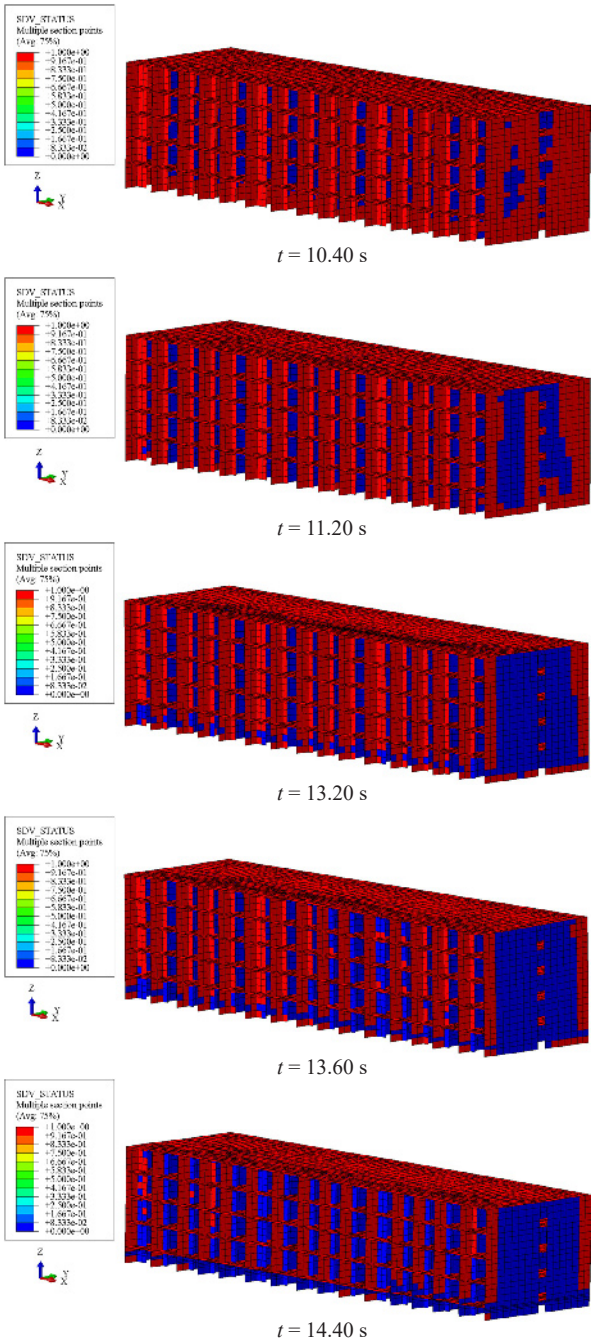

Fig. 14 Damage and collapse of PSRCW for different duration of the earthquake at 0.45 g

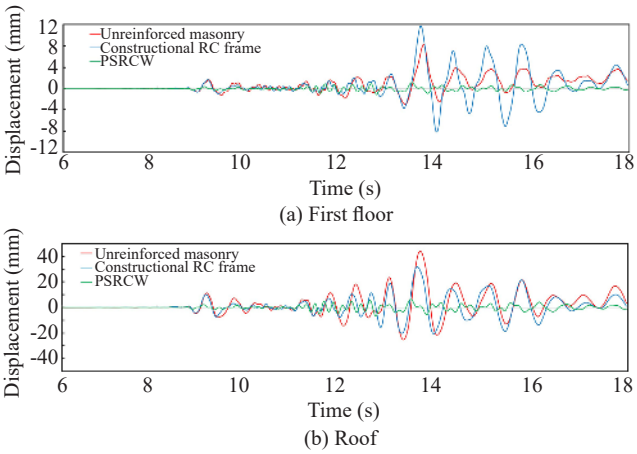

Fig. 15 Displacement histories in *X*-direction

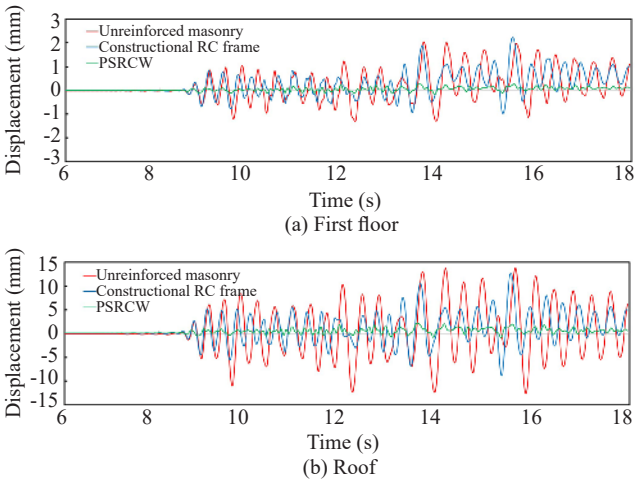

Fig. 16 Displacement histories in *Y*-direction

Table 5 Inter-story drift ratio in *X*-direction

Floor	Unreinforced masonry	Constructional RC frame	PSRCW
1	1/362	1/254	1/2506
2	1/282	1/381	1/1547
3	1/270	1/435	1/1743
4	1/296	1/549	1/2655
5	1/538	1/1158	1/4942

direction. Therefore, the effectiveness of the retrofitting measures in this direction are compared. From the numerical models, it is possible to extract the base shear force sustained by the masonry part for the comparison, as shown in Fig. 17. The maximum force sustained by the masonry part in the PSRCW is about 4.0×10^3 kN, while it is 8.0×10^3 kN and 8.3×10^3 kN for the unreinforced masonry and the constructional RC frame, respectively. PSRCW takes most of the shear force, and the force sustained by the masonry decreased by 50%.

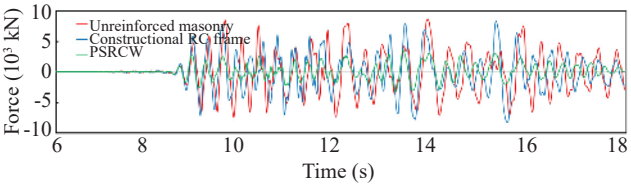

Fig. 17 Base shear forces taken by existing masonry part in *Y*-direction

4.4 Collapse margin analysis

The collapse probability curves of the unreinforced masonry, constructional RC frame and PSRCW are shown in Fig. 16. In this study, the structural subsequent life period is 30 years, so that the PGA of the MCE is 0.30 g. PGAs corresponding to 10% collapse probability for these three structures are 0.15 g, 0.18 g and 0.30 g, respectively, while for 50% collapse probability are 0.19 g, 0.24 g and 0.43 g, and the CMR are 0.65, 0.79 and 1.42, respectively. A CMR of less than 1.0 means the unreinforced masonry and the constructional RC frame cannot meet the requirement of the seismic design code. FEMA P695 also suggests that "the probability of collapse under strong earthquakes shall be less than 10%, which means that the structure meets the requirements for a large earthquake performance". As shown in Fig. 16, when the collapse probability is 10%, the CMR of the PSRCW is equal to 1, which means it just meet the target of seismic fortification for 30 years of subsequent service life. When the PGA reaches 0.30 g, only local partial collapse was observed in the existing masonry structure, but the entire PSRCW remain stable. When the PGA exceeds 0.40 g, with only three out of 42 working conditions, the overall structural collapse happened while in other working conditions, only the middle part of the longitudinal walls was seriously damaged.

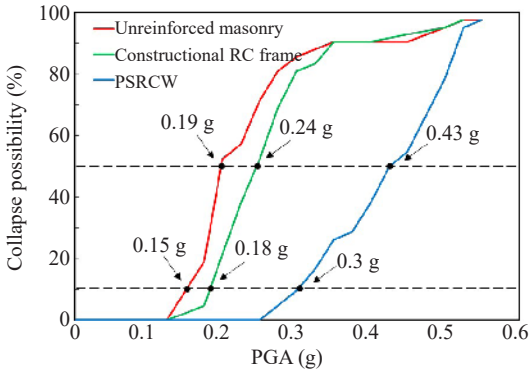

Fig. 18 Collapse probability curves for three structures

5 Conclusion

This study proposed a seismic collapse simulation method for masonry buildings. The local failure and even the collapse of the entire structure is realized through the deactivation of the Gauss integration point both in fiber beam elements and composite layered shell elements. A pseudo rebar layer method is proposed to maintain the damaged composite layered shell element so that the mass exists throughout the analysis and the risk of computation breakdown can be bypassed. Using this method, the collapse performance of the URM, constructional RC frame and PSRCW were studied. According to the collapse margin definition in FEMA P695, the collapse mode and the collapse margin were identified for the three structures, i.e., URM, constructional RC frame, and PSRCW. Some major findings are given as follows:

(1) Within the subsequent service life of 30 years, unreinforced old masonry buildings are seriously damaged under design basis earthquakes and have a high probability of collapse. They cannot meet the safety requirement of the seismic design code.

(2) The ductility of old masonry buildings is improved if retrofitted by a constructional RC frame. The collapse performance, however, is not significantly increased. The collapse probability is still high under the MCE considered in the subsequent service life of 30 years.

(3) To retrofit old masonry buildings by the PSRCW is a good option, not only because it satisfies the retrofitting objectives stipulated by the code but also offers convenient and green construction methods. The collapse margin in the subsequent service life of 30 years is 1.42. In addition, the collapse probability under the MCE is 10%.

Acknowledgment

This research was funded by the Scientific Research Fund of the Institute of Engineering Mechanics, CEA (2016A06), the National Key R&D Program of China under Grant Nos. (2016YFC0701101, 2017YFC1500701), and the National Natural Science Foundation of China (51678538). Any opinions, findings, and conclusion or recommendation expressed herein are those of the authors and do not necessarily reflect the views of the sponsors.

References

Cai JF (1984), *Seismic Damage of Multi-Story Masonry Buildings in Tangshan*, Tsinghua University Press, Beijing, China. (in Chinese)

Caliò I, Marletta M and Pantò B (2012), "A New Discrete Element Model for the Evaluation of the Seismic Behaviour of Unreinforced Masonry Buildings," *Engineering Structures*, **40**: 327–338.

Charleson A and Blondet M (2012), "Seismic Reinforcement for Adobe Houses with Straps from Used Car Tires," *Earthquake Spectra*, **28**(2): 511–530.

Chen ZY (2009), *Disaster and Countermeasures of Buildings During Wenchuan Earthquake*, China Building Industry Press, Beijing, China. (in Chinese)

Dai J, Qu Z, Zhang C and Weng X (2013), "Preliminary Investigation of Seismic Damage to Two Steel Space Structures During The 2013 Lushan Earthquake," *Earthquake Engineering and Engineering Vibration*, **12**(3): 497–500.

ElGawady M, Lestuzzi P and Badoux M (2004), "A Review of Conventional Seismic Retrofitting Techniques for URM," *13th Brick & Block Masonry Conf.*, Amsterdam, **9**: 1–9.

FEMA P695 (2009), "Quantification of building seismic performance factors," *ATC 263 Project Report*.

Gu XL, Peng B, Chen GL, Li X and Ouyang Y (2012), "Rapid Strengthening of Masonry Structures Cracked In Earthquakes Using Fiber Composite Materials," *Journal of Composites for Construction*, ASCE, **16**(5): 590–603.

Hakuno M and Meguro K (1993), "Simulation of Concrete-Frame Collapse due to Dynamic Loading," *Journal of Engineering Mechanics*, **119**(9): 1709–1723.

Lemos JV (2007), "Discrete element Modeling of Masonry Structures," *International Journal of Architectural Heritage*, **1**(2): 190–213.

Li J (2013), "The Collapsed Factors Analysis of Masonry Structures and Preliminary Exploration about Anti-collapse Based Numerical Simulation," *Master Dissertation*, Chongqing University. (in Chinese)

Li WF, Wang T, Chen X, Zhong X and Pan P (2017), "Pseudo-Dynamic Tests on Masonry Residential Buildings Seismically Retrofitted by PSRCWs," *Earthquake Engineering and Engineering Vibration*, **16**(3): 587–597.

Lu X, Lu XZ, Guan H, *et al*. (2013), "Collapse Simulation of Reinforced Concrete High-Rise Building Induced by Extreme Earthquakes," *Earthquake Engineering and Structural Dynamics*, **42**(5):705–723.

Ministry of Housing and Urban-Rural Development of China (2010), *Code for Design of Concrete Structures* (*GB 50010-2010*), China Architecture and Building Press, Beijing, China. (in Chinese)

Ministry of Housing and Urban-Rural Development of China (2011), *Code for Design of Masonry Structures* (*GB 50003-2011*), China Architecture and Building Press, Beijing, China. (in Chinese)

Ministry of Housing and Urban-Rural Development of China (2016), *Code for Seismic Design of Buildings* (*GB 50011-2010*), China Architecture and Building Press, Beijing, China. (in Chinese)

Moon FL, Yi TY, Leon R and Kahn L (2007), "Testing of A Full-Scale Unreinforced Masonry Building Following Seismic Strengthening," *Journal of Structural Engineering*, ASCE, **133**(9): 1215–1226.

Standardization Administration of The People's Republic of China (2015), *Seismic Ground Motion Parameters Zonation Map of China* (*GB 18306-2015*), Standards Press of China, Beijing, China. (in Chinese)

Su QW, Xu H, Wu H, Zhang Y and GQ (2013), "Research on Inter-Story Displacement Angle of Brick Masonry Structures," *China Civil Engineering Journal*, **46**(S1): 26–32.

Sun BT and Yan PL (2015), "Damage Characteristics and Seismic Capacity of Buildings During Nepal M_s 8.1 Earthquake," *Earthquake Engineering and Engineering Vibration*, **14**(3): 571–578.

Taghdi M, Bruneau M and Saatcioglu M (2000), "Seismic Retrofitting of Low-Rise Masonry and Concrete Walls Using Steel Strips," *Journal of Structural Engineering*, ASCE, **126**(9): 1017–1025.

Vamvatsikos D and Cornell CA (2002), "Incremental dynamic analysis," *Earthquake Engineering and Structural Dynamics*, **31**(3): 491–514.

Wang T, Cheng C and Guo X (2012), "Model-Based Predicting and Correcting Algorithms for Substructure Online Hybrid Tests," *Earthquake Engineering and Structural Dynamics*, **41**(15): 2331–2349.

Wang T and Nakashima M (2013), "Flexible Substructure Online Hybrid Test System Using Conventional Testing Devices," *Earthquake Engineering and Engineering Vibration*, **12**(3): 341–350.

Xu Hu (2008), "Analysis on Seismic Collapse Resistant Behavior of the Large-Bay Multistory Brick Masonry Structures," *Doctor Dissertation*, Southwest Jiaotong University. (in Chinese)

Zheng KY (2012), "Seismic Collapse Study of Masonry Walls and Structures," *Master Dissertation*, Hunan University. (in Chinese)